Radiometer Considerations

Lectures in Maratea
22 – 31 May 2003

Paul Menzel
NOAA/NESDIS/ORA

Relevant Material in Applications of Meteorological Satellites

Remote Sensing Instrument Considerations

Radiometer Components

Optics	collect incoming radiation
	separate or disperse the spectral components
	(dichroics, grating spectrometer, interferometer, prism,...)
	focus the radiation to field stop
Detectors	respond to the photons with a voltage signal
Electronics	voltage signal is amplified by the electronics
	A/D converts into digital counts.

Performance Characteristics

Responsivity	measure of the output per input
Detectivity	ratio of the responsivity per noise voltage
Calibration	attempts to reference the output to known inputs.

Design Considerations

Diffraction	function of the mirror size
Impulse Response	determines how sharp edges appear
Signal to Noise	how clean is the image
Infrared Calibration	enables quantitative use of measurements
Bit Depth	truncation error can limit precision of data

Satellite Orbits

Geostationary vs Polar orbiting vs Other

Approaches To Separate Radiation into Spectral Bands

radiometer - uses filters to separate spectrum by reflection and transmission (wavelengths are selectively reflected and transmitted)

prism - separates spectrum by refraction (different wavelengths bend into different paths)

grating spectrometer - spatially separates spectrum by diffraction (wavelets from different slits will be in phase in different locations depending on wavelength)

interferometer - separates spectrum by interference patterns spread out temporally (wavelets from different paths will be in phase at different times depending on wavelength)

Separation of Spectra

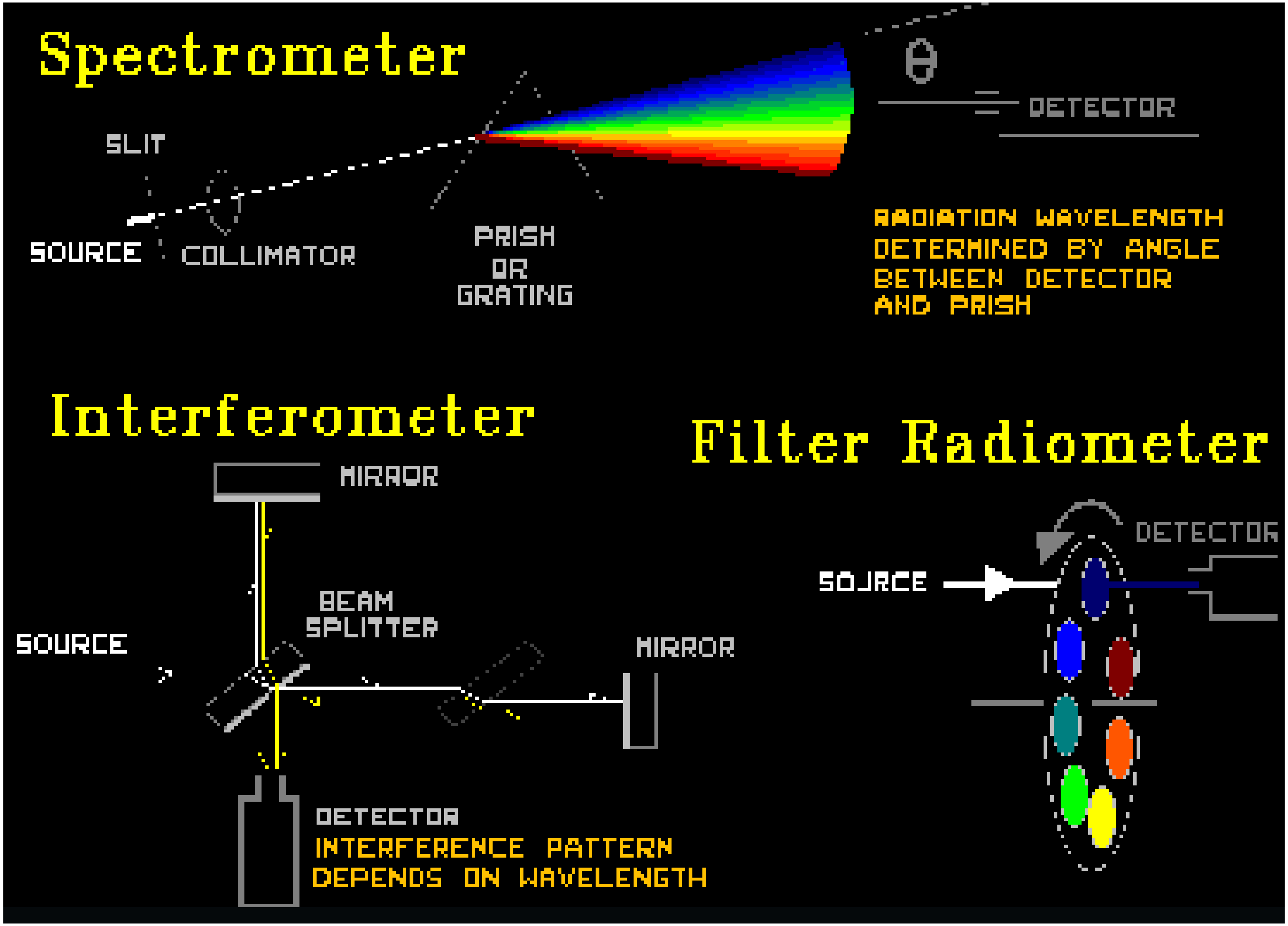

Spectral Separation with a Prism: longer wavelengths deflected less

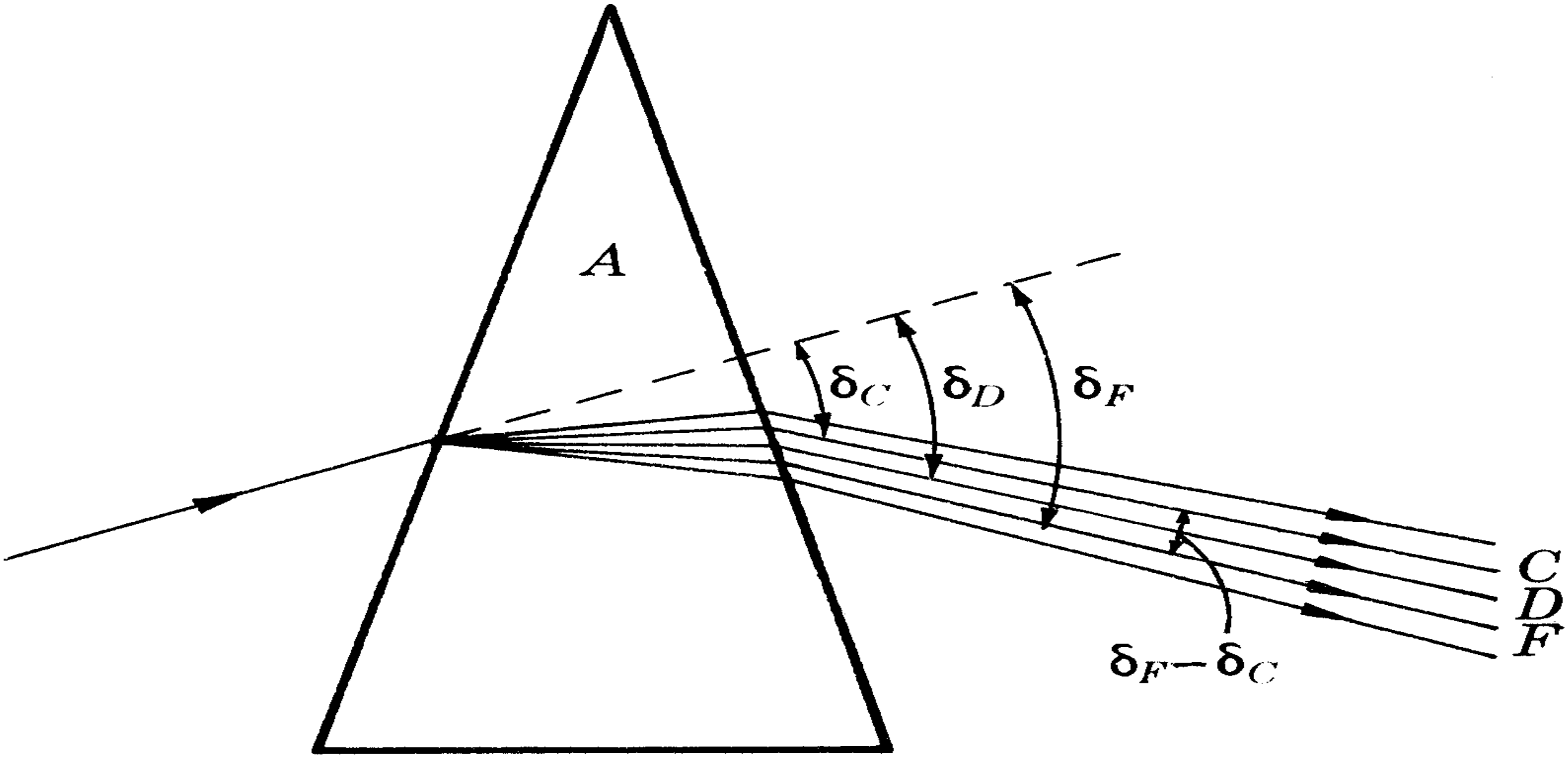

Spectral Separation with a Grating: path difference from slits produces positive and negative wavelet interference on screen

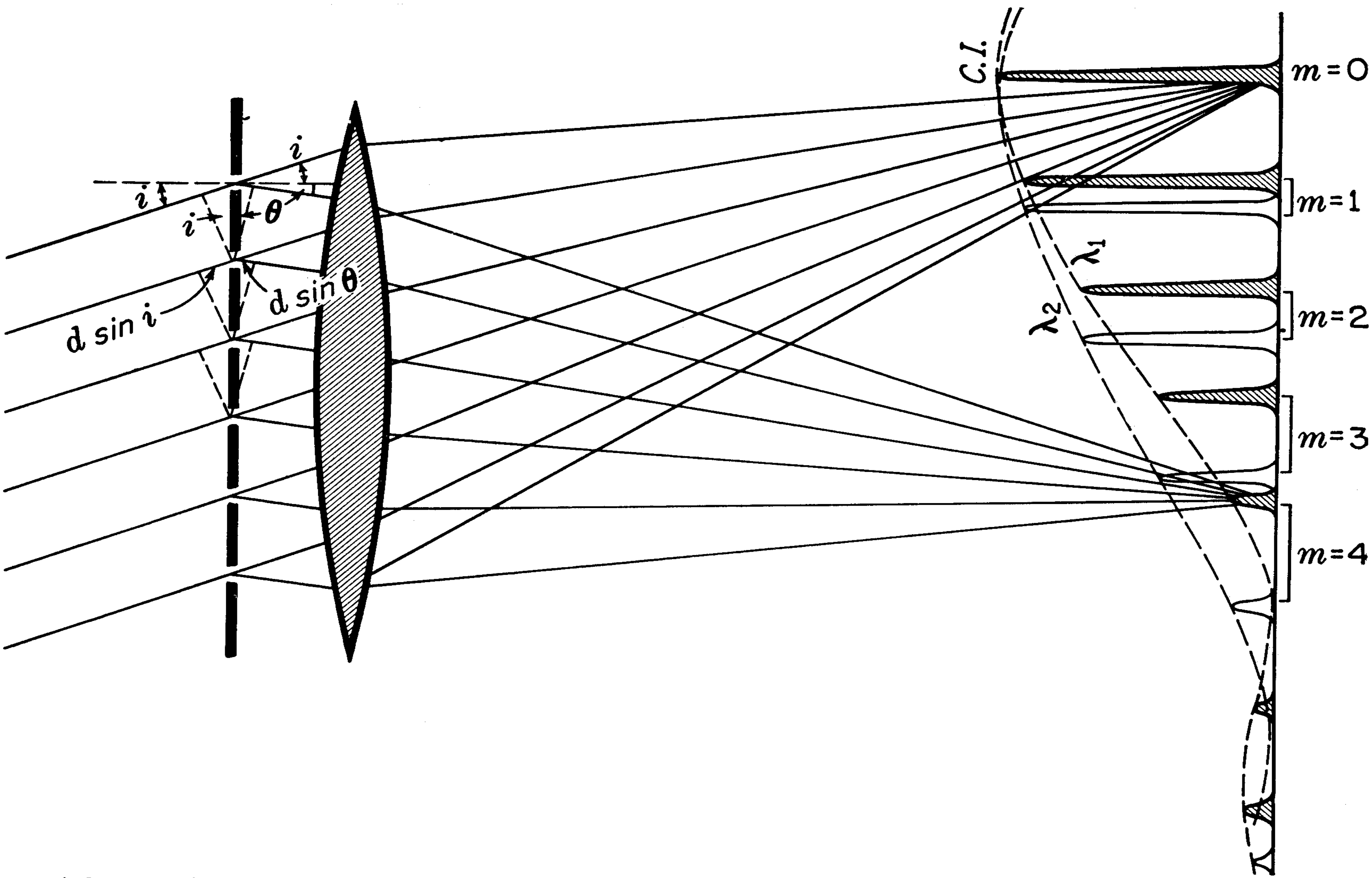

<u>Spectral Separation with an Interferometer</u> - path difference (or delay) from two mirrors produces positive and negative wavelet interference

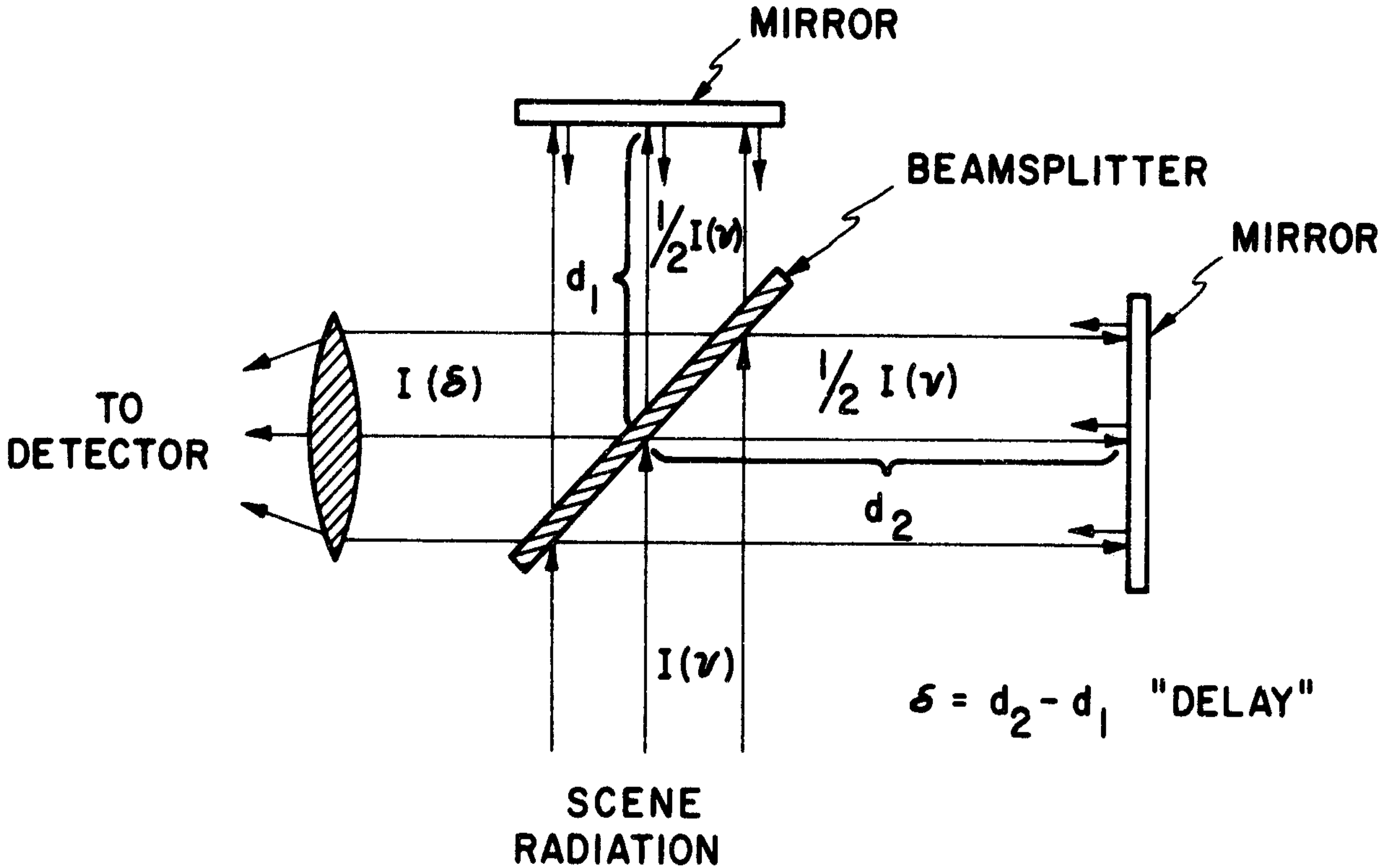

Design Considerations (1)

Diffraction

Mirror diameter defines ability of radiometer to resolve two point sources on the earth surface. Rayleigh criterion indicates that angle of separation , θ, between two points just resolved (maxima of diffraction pattern of one point lies on minima of diffraction pattern of other point)

$$\sin \theta = \lambda / d$$

where d is diameter of mirror and λ is wavelength. Geo satellite mirror diameter of 30 cm at infrared window wavelengths (10 microns) has resolution of about 1 km. This follows from

$$10\text{-}5 \text{ m} / 3 \times 10\text{-}1 \text{ m} = 3.3 \times 10\text{-}5 = r / 36{,}000 \text{ km}$$

or

$$r = 1 \text{ km} = \text{resolution.}$$

Energy distribution from diffraction through a circular aperture

Max number	energy	location of ring
Central max	E	$0 \rightarrow 1.22\ \lambda / d$
Second max	0.084E	$1.22 \rightarrow 2.23\ \lambda / d$
Third max	0.033E	$2.23 \rightarrow 3.24\ \lambda / d$
Fourth max	0.018E	$3.24 \rightarrow 4.24\ \lambda / d$
Fifth max	0.011E	$4.24 \rightarrow 5.24\ \lambda / d$

Thus for a given aperture size more energy is collected within a given FOV size for shorter vs. longer wavelengths

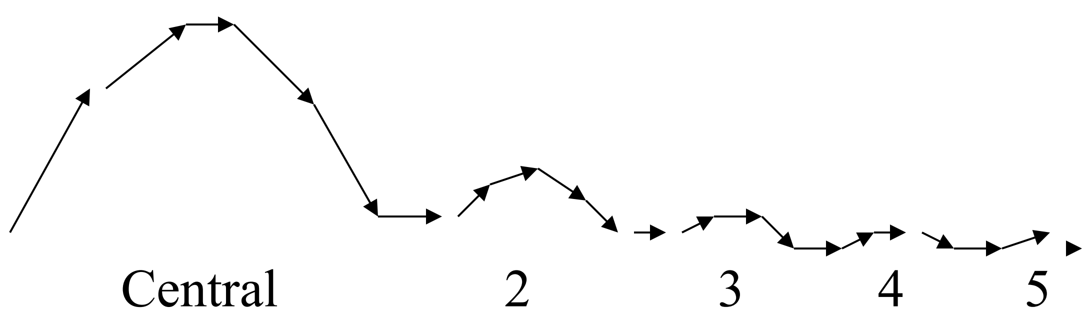

Energy distribution of 4 micron radiation going through a geo 30 cm diameter circular aperture to the focal point

Max number	% Energy	radius of source
Central max	82%	0.58 km
Second max	91%	1.06 km
Third max	94%	1.54 km
Fourth max	95%	2.02 km
Tenth max	98%	4.88 km
Twentieth max	99%	30.3 km
Fortieth max	99.5%	50.6 km

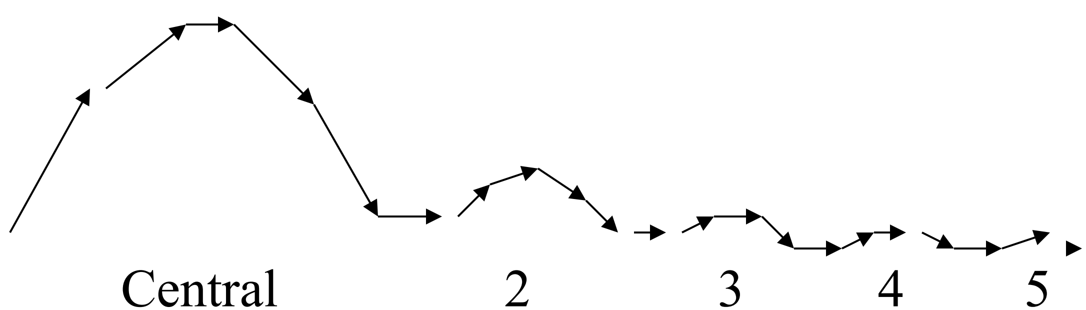

Energy distribution of 10 micron radiation going through a geo 30 cm diameter circular aperture to the focal point

Max number	% Energy	radius of source
Central max	82%	1.45 km
Second max	91%	2.65 km
Third max	94%	3.84 km
Fourth max	95%	5.04 km
Tenth max	98%	12.2 km
Twentieth max	99%	75.7 km
Fortieth max	99.5%	126.4 km

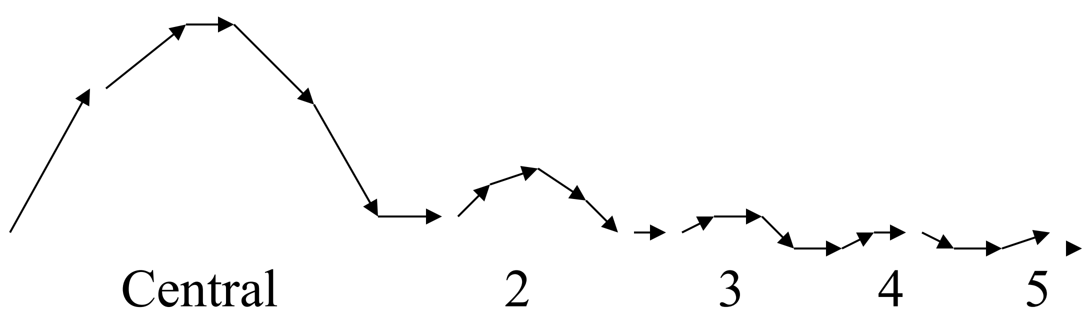

Energy distribution of 10 micron radiation going through a geo 50 cm diameter circular aperture to the focal point

Max number	% Energy	radius of source
Central max	82%	0.84 km
Second max	91%	1.59 km
Third max	94%	2.30 km
Fourth max	95%	3.02 km
Tenth max	98%	7.32 km
Twentieth max	99%	45.4 km
Fortieth max	99.5%	75.8 km

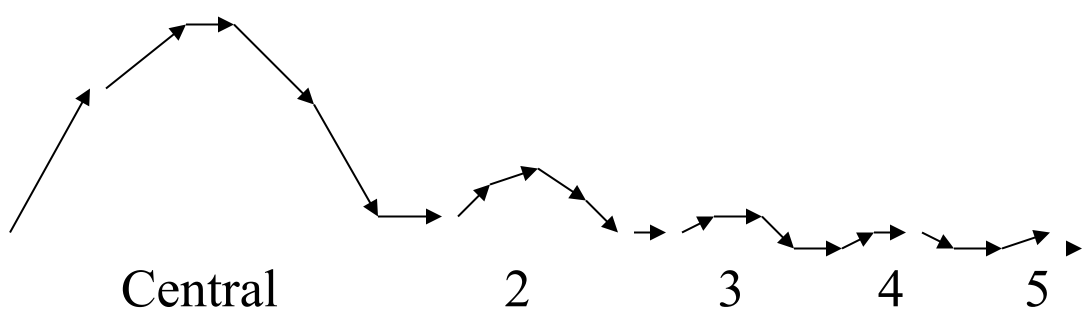

Distribution of 10 um energy sources focused by 30 cm mirror onto 112 urad square detector (total detected signal emanating from circle of given size)

% of signal	emanating from circle with diameter of (FOV = 4km)
60%	one FOV
73%	1.25 FOV
79%	1.5 FOV

Effect of nearby 220 K clouds on 300K clear scene for clear sky brightness temperature (CSBT) to be within 1 K clear area must have at least 30 km diameter

Rule of thumb is 1% 220 K cloud and 99% 300 K clear sky results in CSBT off by 0.5 K at 10 microns

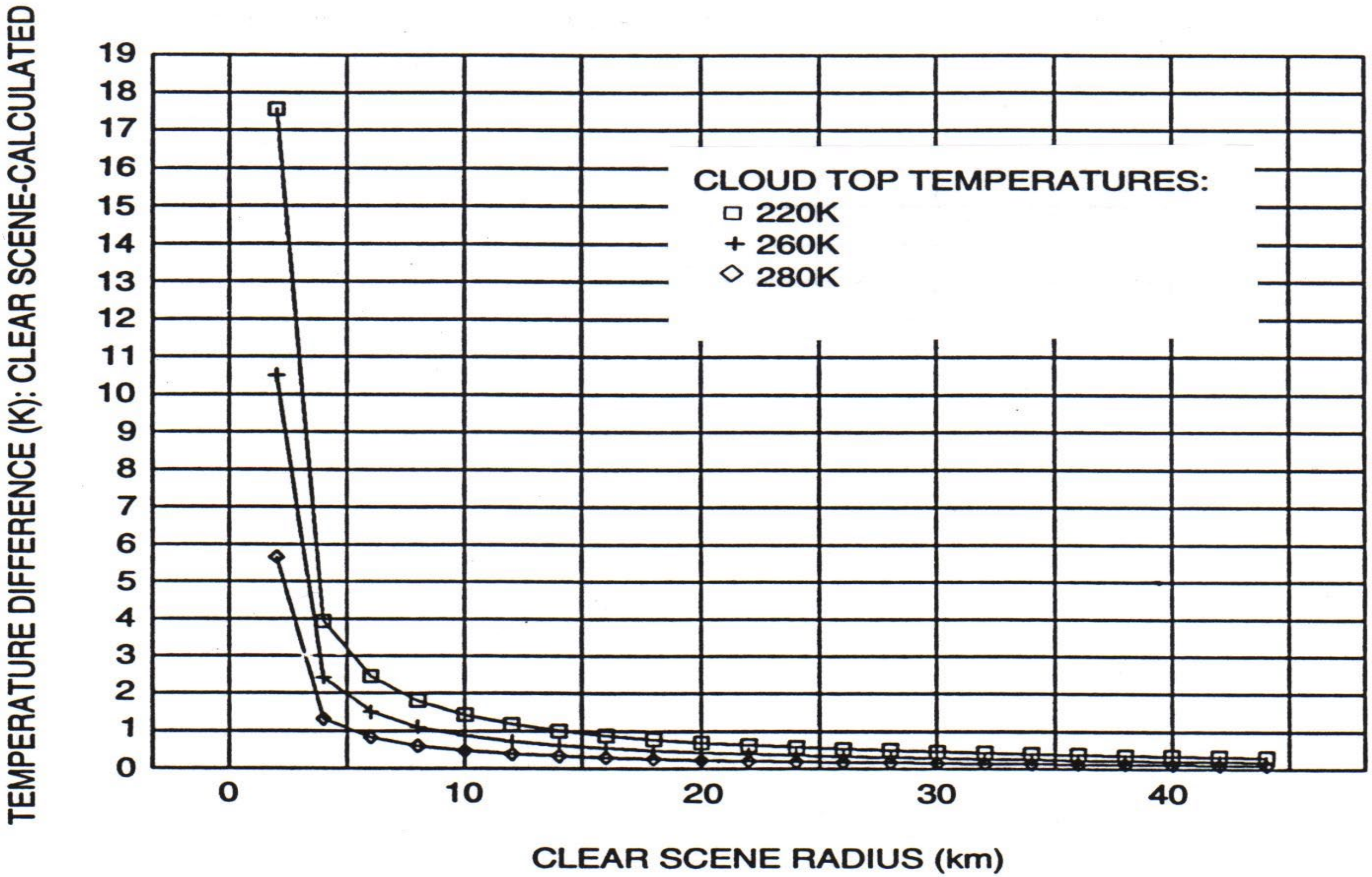

Calculated diffraction effects for Geo 30 cm mirror for infrared window radiation with a 2 km radius FOV in a clear scene of brightness temperature 300 K surrounded by clouds of 220, 260, or 280 K. Brightness temperature of a 10 radius clear hole is too cold by about 1.5 K.

Design Considerations (2)

Impulse or Step Response Function

Detector collects incident photons over a sampling time and accumulates voltage response, which is filtered electronically. This is characterized by impulse (or step) response function, detailing what response of sensor is to delta (or step) function input signal. Response function is determined from characteristics of prealiasing filter which collects voltage signal from detector at sampling times.

Perfect response of detector continuously sampling scene with 100% contrast bar extending one FOV.

Scene radiance

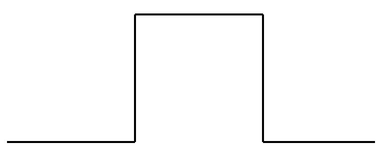

Detector response

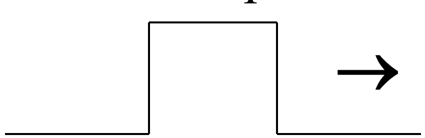

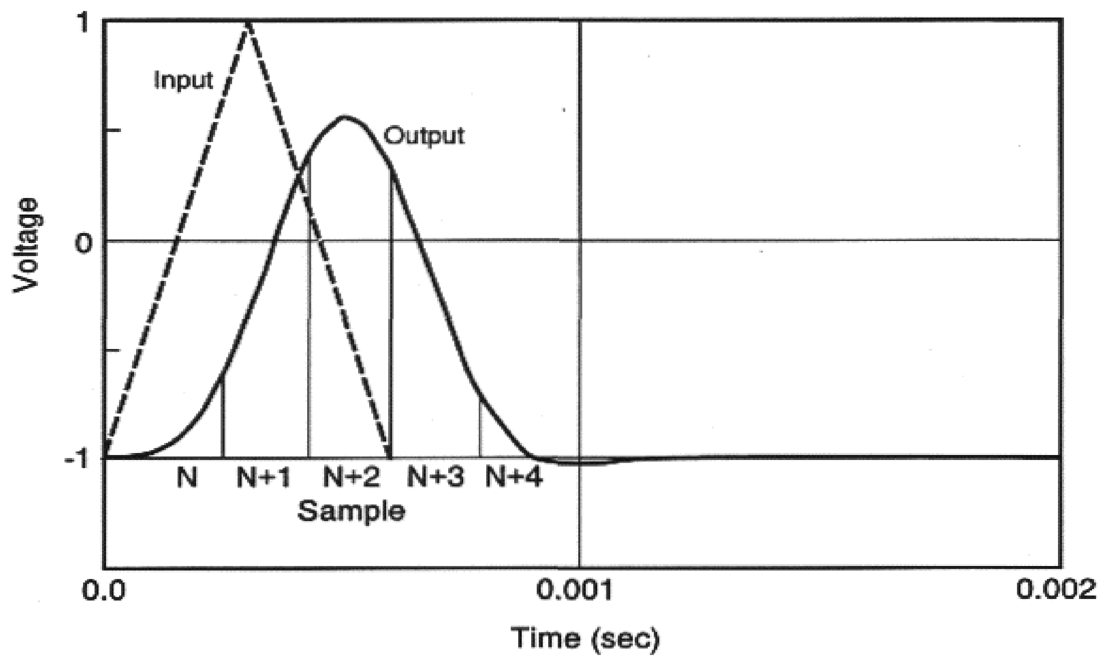

Percentage of total signal appearing in samples preceding and following correlated sample peak; for GOES-8 infrared window samples sample N-2 has 4.3% of total signal, N-1 has 26.5%, N peaks with 44.8%, N+1 has 23.4%, and N+2 has 1.0%. This causes smearing of cloud edges and other radiance gradients.

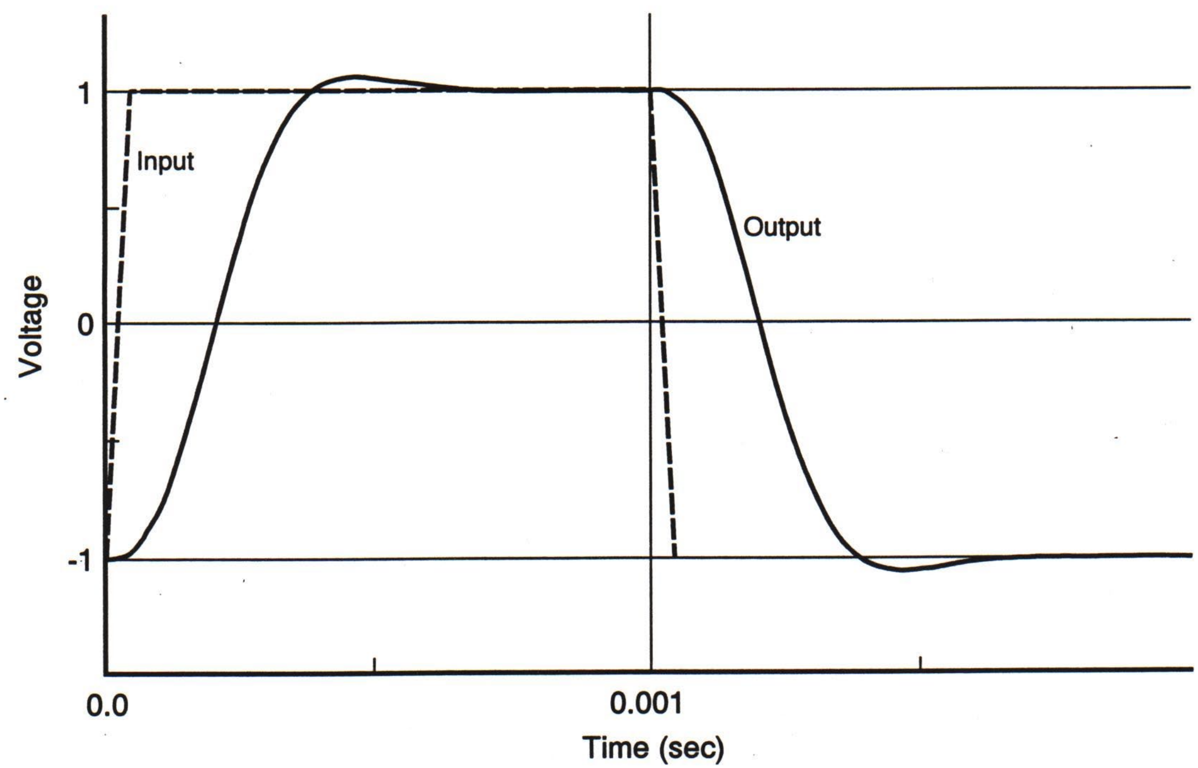

Design Considerations (3)

Detector Signal to Noise

Noise equivalent radiance for infrared detector can be expressed as

$$NEDR(\nu) = \gamma\, [Ad\, \Delta f]^{1/2} / [Ao\, \tau(\Delta\nu)\, \Omega\, D^*\, \Delta\nu]$$

where
- γ is preamplifier degradation factor
- Ad is detector area in cm2
- Δf is effective electronic bandwidth of radiometer
- Ao is mirror aperture area in cm2
- $\tau(\Delta\nu)$ is transmission factor of radiometer optics in spectral interval $\Delta\nu$
- Ω is solid angle of FOV in steradians
- D^* is specific spectral detectivity of detector in spectral band in cm $Hz^{1/2}$ / watt, and
- $\Delta\nu$ is spectral bandwidth of radiometer at wavenumber ν in cm-1.

NEDR for GOES-8 imager

Band	Wavelength (micron)	Detector	NEDR (mW/m2/ster/cm-1)	NEDT
1	.52 - .75	Silicon	(3 of 1023 counts is noise)	
2	3.83-4.03	InSb	0.0088	0.23 @ 300 K
3	6.5 - 7.0	HgCdTe	0.032	0.22 @ 230 K
4	10.2-11.2	HgCdTe	0.24	0.14 @ 300 K
5	11.5-12.5	HgCdTe	0.45	0.26 @ 300 K

Design Considerations (4)

Infrared Calibration

Radiometer detectors are assumed to have linear response to infrared radiation, where target output voltage is given by

$$Vt = \alpha Rt + Vo$$

and Rt is target input radiance, α is radiometer responsivity, and Vo is system offset voltage. Calibration consists of determining α and Vo. This is accomplished by exposing radiometer to two different external radiation targets of known radiance. A blackbody of known temperature and space (assumed to emit no measurable radiance) are often used as the two references. If z refers to space, bb blackbody, calibration can be written as

$$Vz = \alpha Rz + Vo$$
$$Vbb = \alpha Rbb + Vo$$

where

$$\alpha = [Vbb - Vz]/[Rbb - Rz]$$
$$Vo = [Rbb\, Vz - Rz\, Vbb]/[Rbb - Rz]$$

Using Rz=0 this yields

$$Rt = Rbb\, [Vt - Vz] / [Vbb - Vz].$$

Design Considerations (5)

Bit Depth

Range of radiances expected for earth and atmosphere in a given spectral band must be converted to digital counts of fixed bit depth. This introduces truncation error. For n bit data, the radiance range, must be covered in 2^n even increments. GOES-8 imager truncation errors are indicated below.

Band	λ	Bit Depth	Rmax	ΔR	Tmax	ΔT(230)	ΔT(300)
	(micron)		(mW/m2/ster/cm-1)			(degrees Kelvin)	
1	.65	10			(better detail in images)		
2	3.9	10	3.31	0.003	335	2.14	0.09
3	6.7	10	48.3	0.047	320	0.33	0.06
4	10.7	10	147.7	0.144	320	0.20	0.09
5	12.0	10	166.5	0.163	320	0.19	0.09

Examples from MODIS

Instrument configuration

Qualitative radiance considerations

IR Cal Val

NEDR

Image artifacts

TPW product validation

MODIS SCAN CAVITY

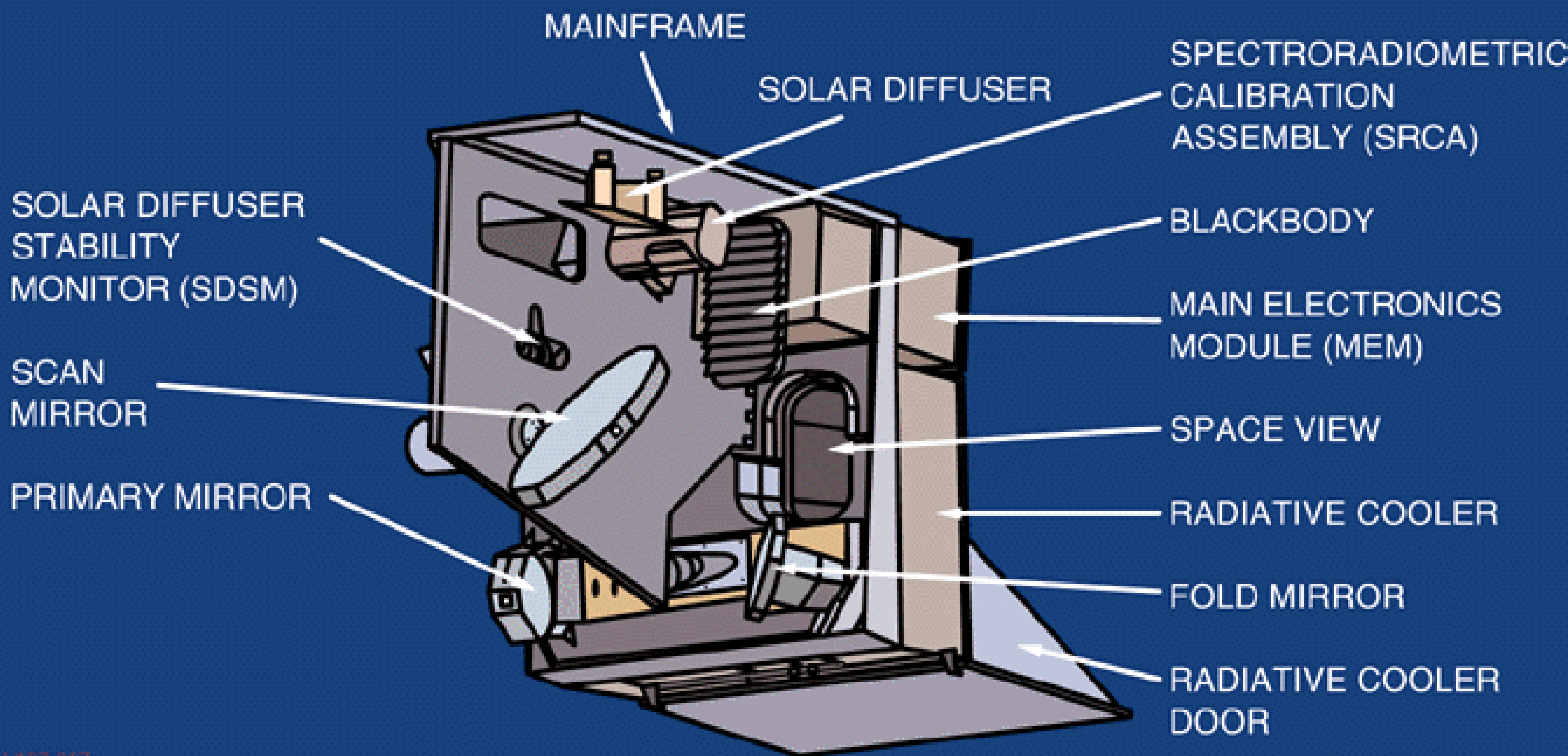

Atmospheric Profile Retrieval from MODIS Radiances

$$I_\lambda = \varepsilon_\lambda^{sfc} B_\lambda(T(p_s))\, \tau_\lambda(p_s) - \int_o^{p_s} B_\lambda(T(p))\, [\, d\tau_\lambda(p) / dp \,]\, dp\, .$$

I1, I2, I3, ... , In are measured with MODIS
P(sfc) and T(sfc) come from ground based conventional observations
$\tau_\lambda(p)$ are calculated with physics models

Regression relationship is inferred from (1) global set of in situ radiosonde reports, (2) calculation of expected radiances, and (3) statistical regression of observed raob profiles and calculated MODIS radiances

Need RT model, estimate of $\varepsilon_\lambda^{sfc}$, and MODIS radiances

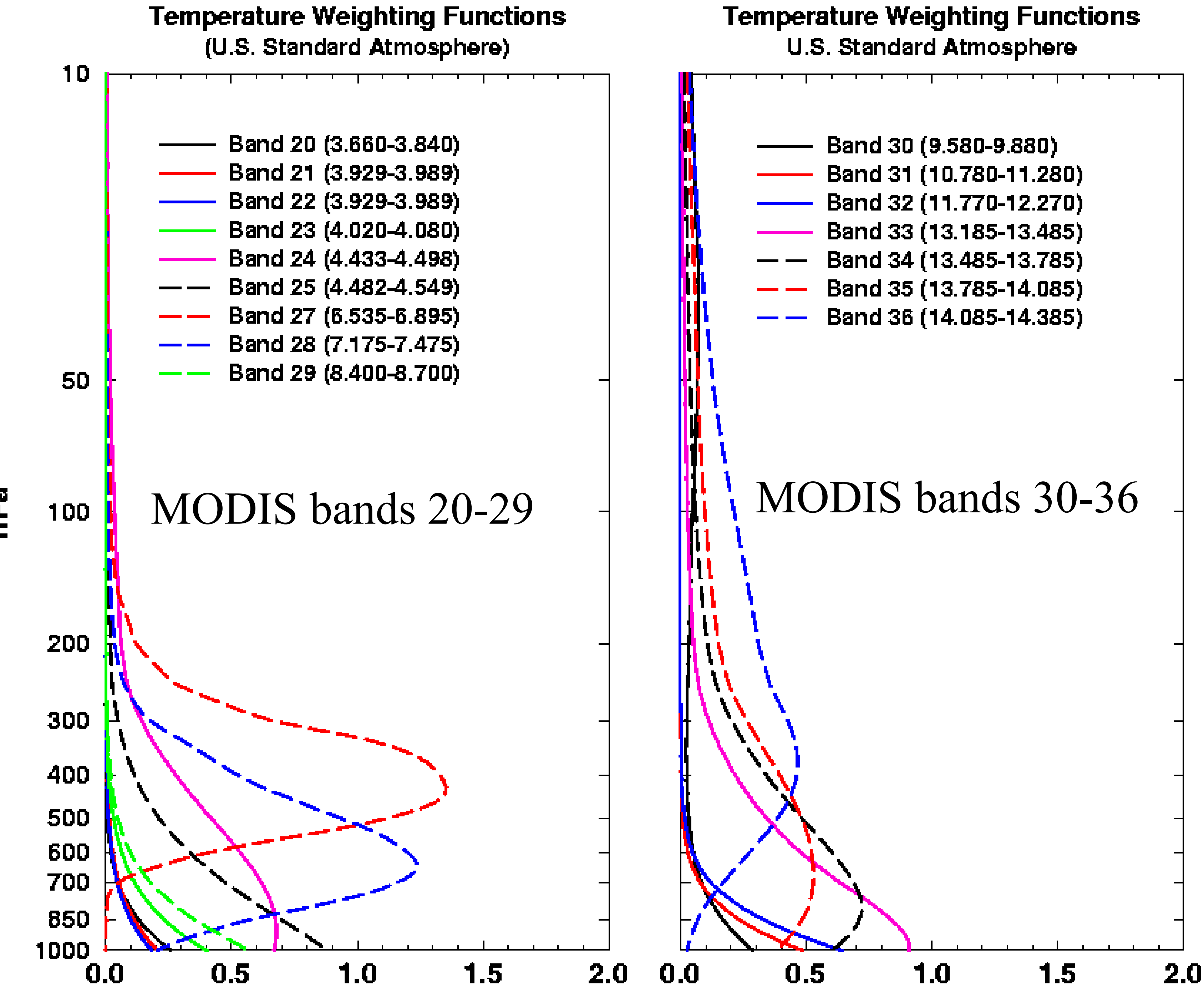
Temperature Weighting Functions
(U.S. Standard Atmosphere)
Band 20 (3.660-3.840)
Band 21 (3.929-3.989)
Band 22 (3.929-3.989)
Band 23 (4.020-4.080)
Band 24 (4.433-4.498)
Band 25 (4.482-4.549)
Band 27 (6.535-6.895)
Band 28 (7.175-7.475)
Band 29 (8.400-8.700)
MODIS bands 20-29
10
50
100
200
300
400
500
600
700
850
1000
0.0
0.5
1.0
1.5
2.0
Temperature Weighting Functions
U.S. Standard Atmosphere
Band 30 (9.580-9.880)
Band 31 (10.780-11.280)
Band 32 (11.770-12.270)
Band 33 (13.185-13.485)
Band 34 (13.485-13.785)
Band 35 (13.785-14.085)
Band 36 (14.085-14.385)
MODIS bands 30-36
0.0
0.5
1.0
1.5
2.0

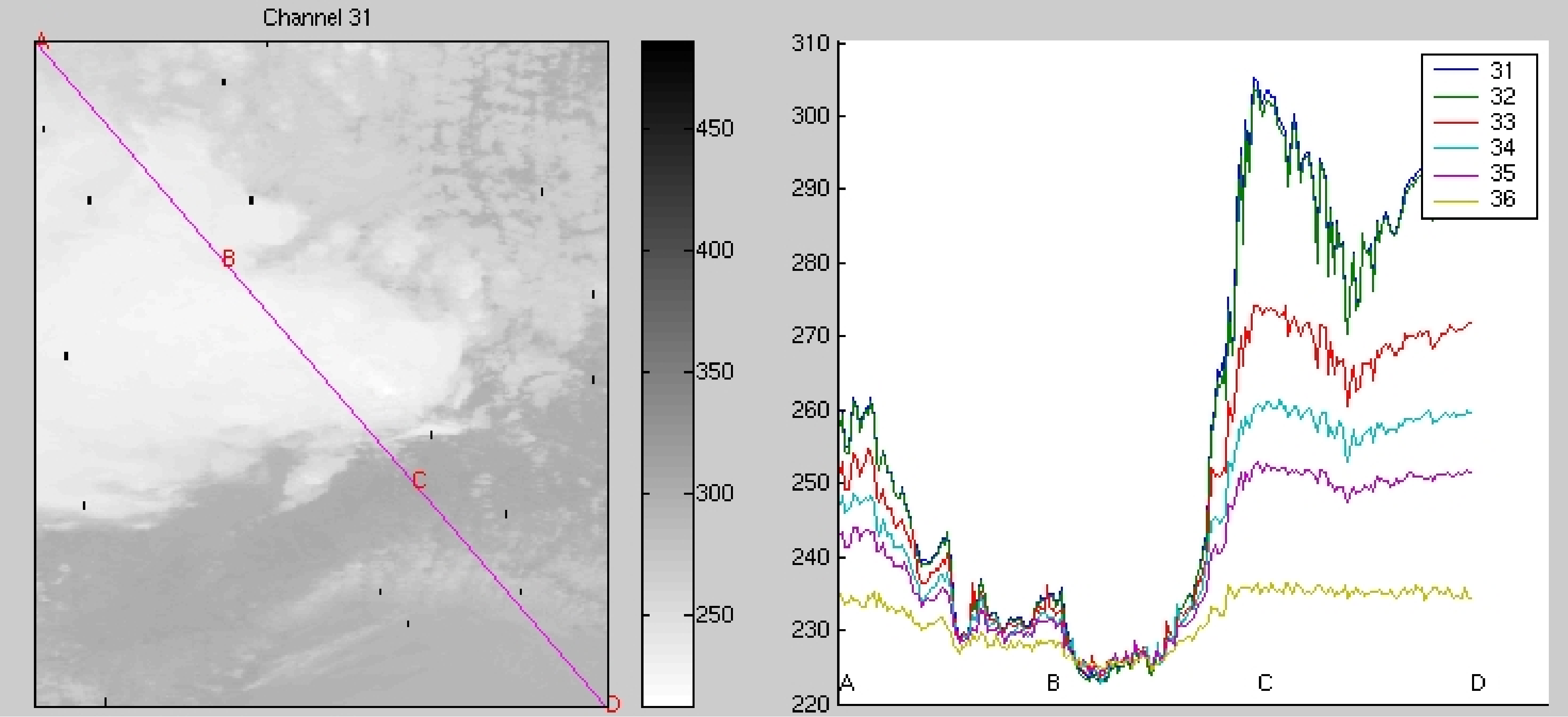

Channel 31
A
B
C
D
450
400
350
300
250
310
300
290
280
270
260
250
240
230
220
31
32
33
34
35
36

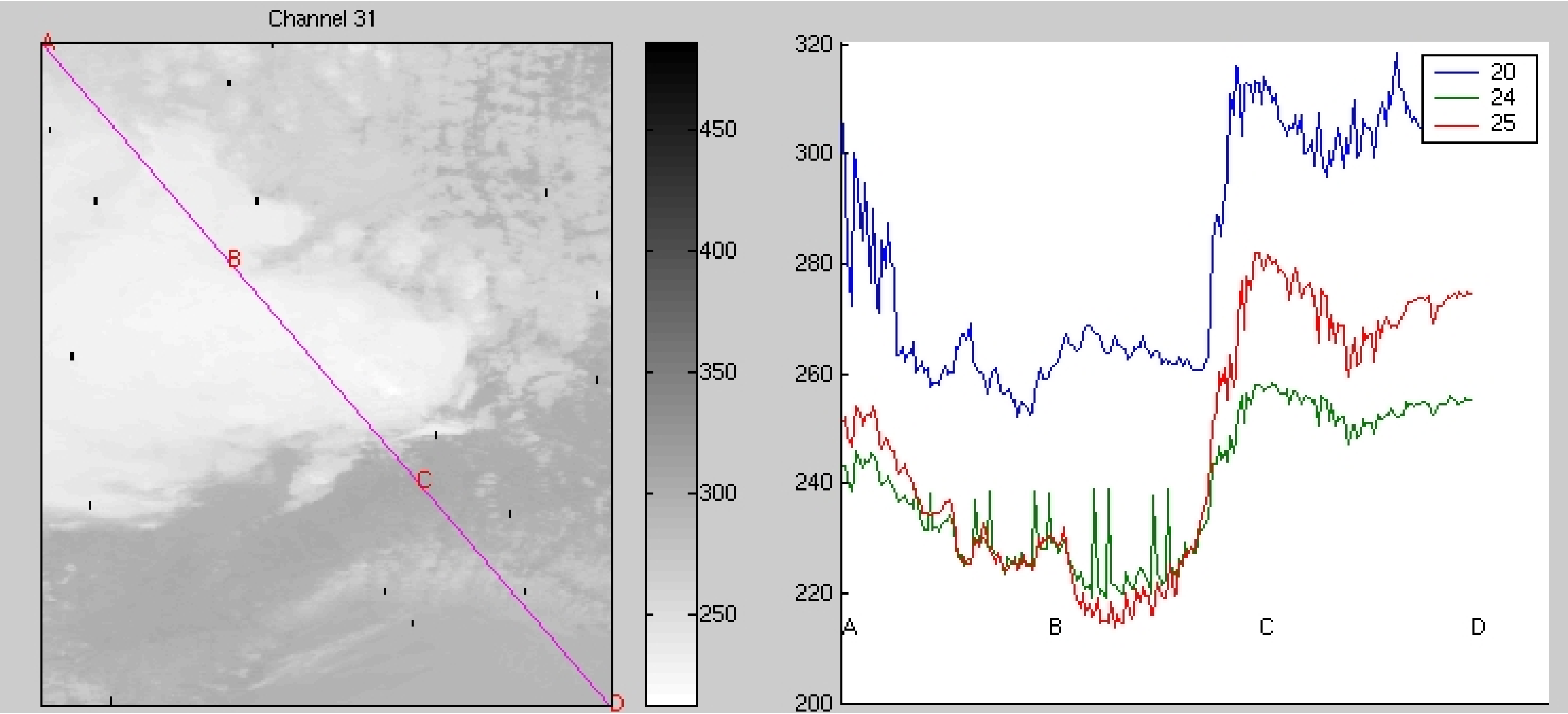

Channel 31
A
B
C
D
450
400
350
300
250
320
300
280
260
240
220
200
20
24
25
A
B
C
D

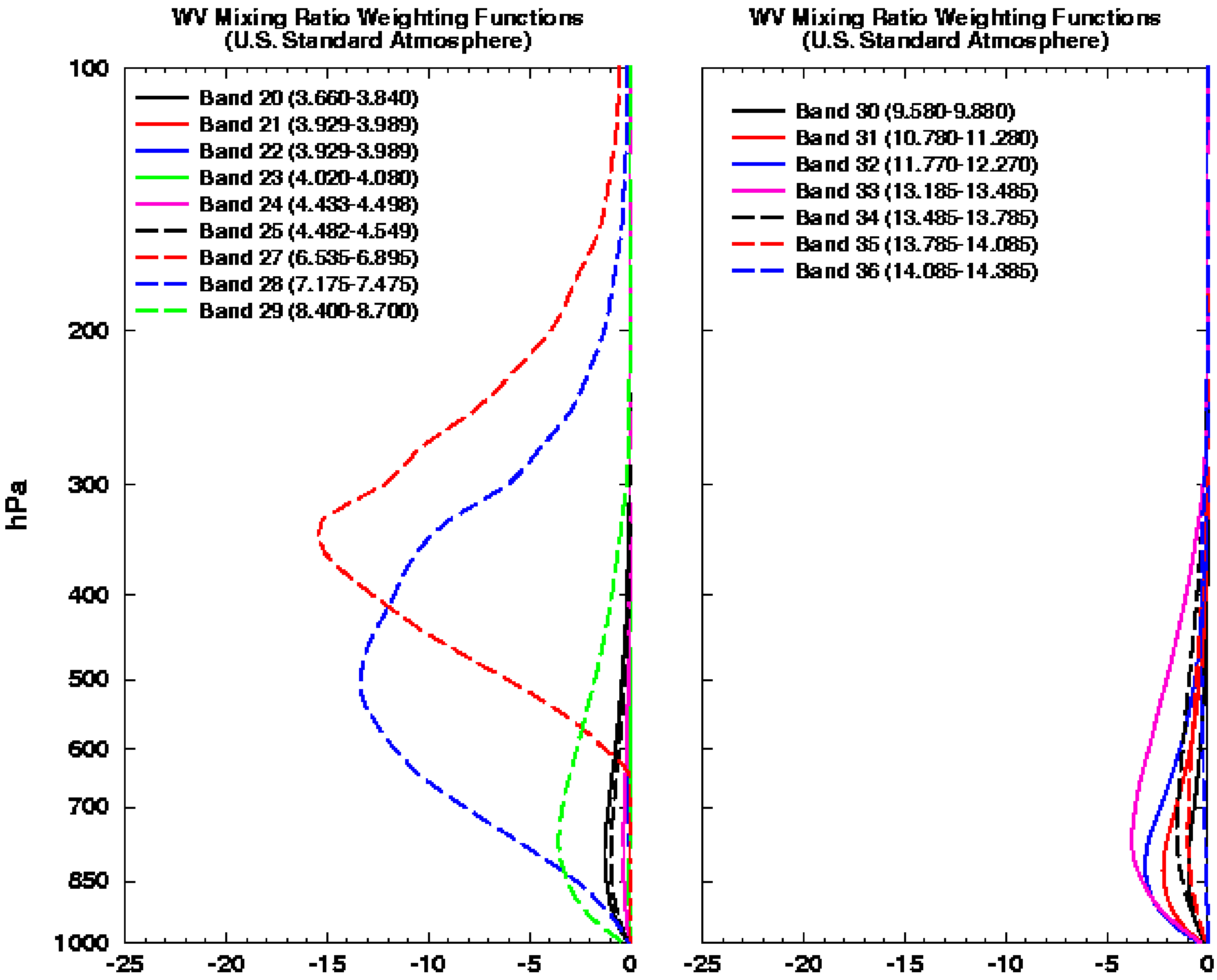
WV Mixing Ratio Weighting Functions
(U.S. Standard Atmosphere)
hPa
100
200
300
400
500
600
700
850
1000
Band 20 (3.660-3.840)
Band 21 (3.929-3.989)
Band 22 (3.929-3.989)
Band 23 (4.020-4.080)
Band 24 (4.433-4.498)
Band 25 (4.482-4.549)
Band 27 (6.535-6.895)
Band 28 (7.175-7.475)
Band 29 (8.400-8.700)
-25
-20
-15
-10
-5
0
WV Mixing Ratio Weighting Functions
(U.S. Standard Atmosphere)
Band 30 (9.580-9.880)
Band 31 (10.780-11.280)
Band 32 (11.770-12.270)
Band 33 (13.185-13.485)
Band 34 (13.485-13.785)
Band 35 (13.785-14.085)
Band 36 (14.085-14.385)
-25
-20
-15
-10
-5
0

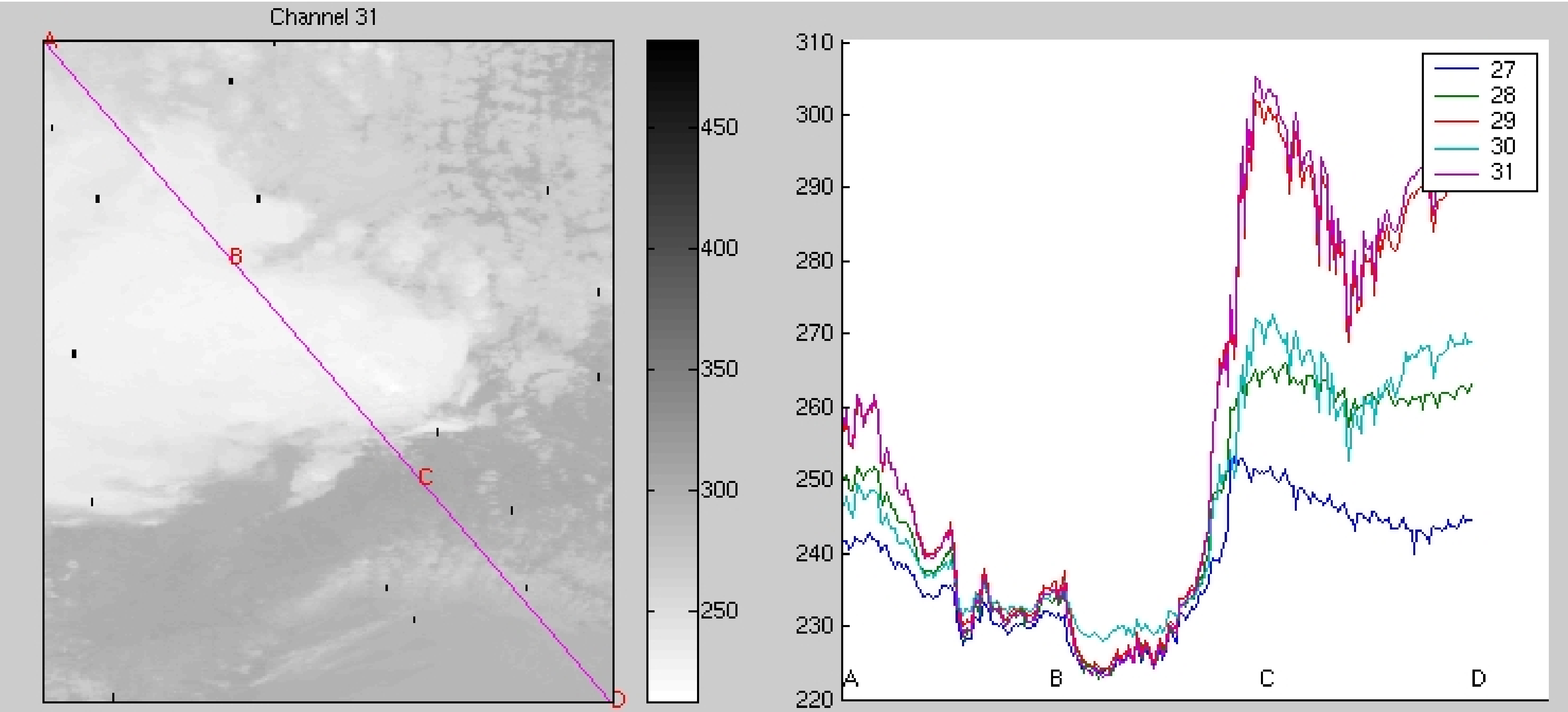

Channel 31
A
B
C
D
450
400
350
300
250
310
300
290
280
270
260
250
240
230
220
27
28
29
30
31

MODIS Emissive Band Cal/Val from ER-2 Platform

- Transfer S-HIS cal to MAS
- Co-locate MODIS FOV on MAS
- Remove spectral, geometric dependence
- WISC-T2000, SAFARI-2000, TX-2001

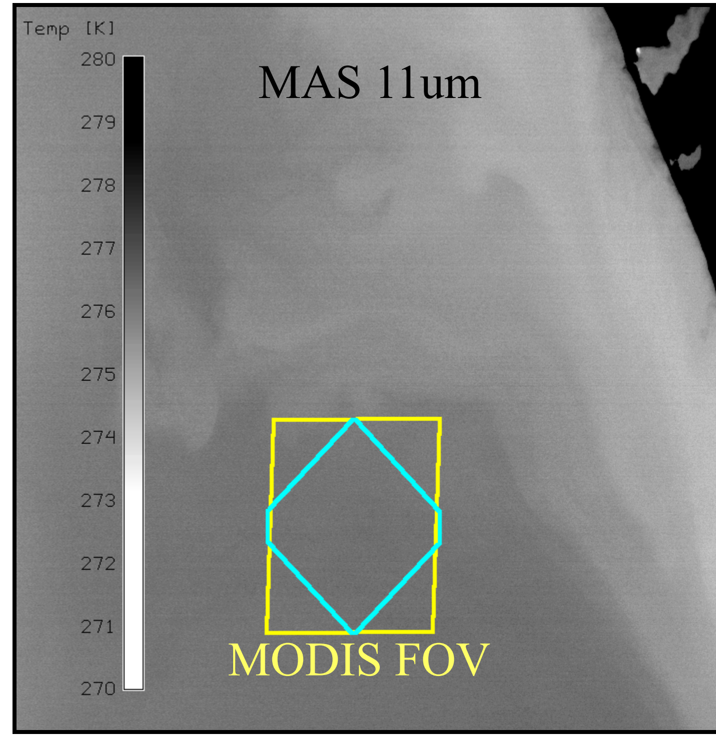

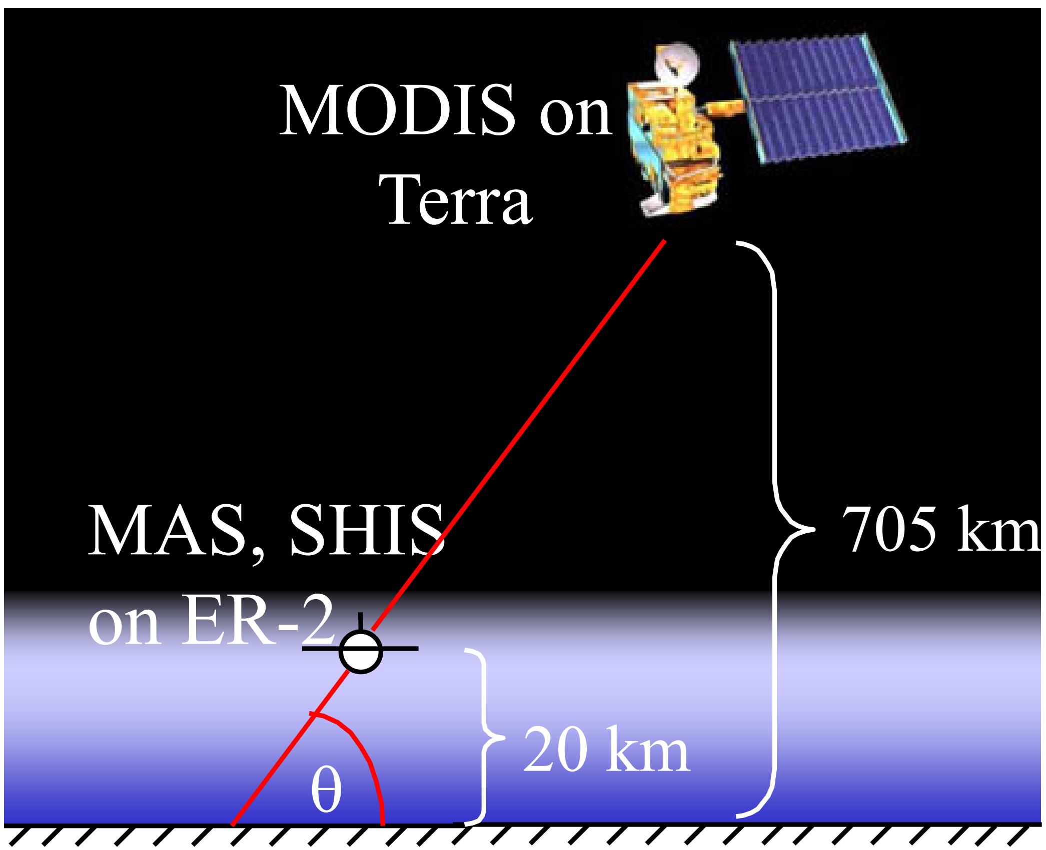

MODIS L1B Accuracy Assessment

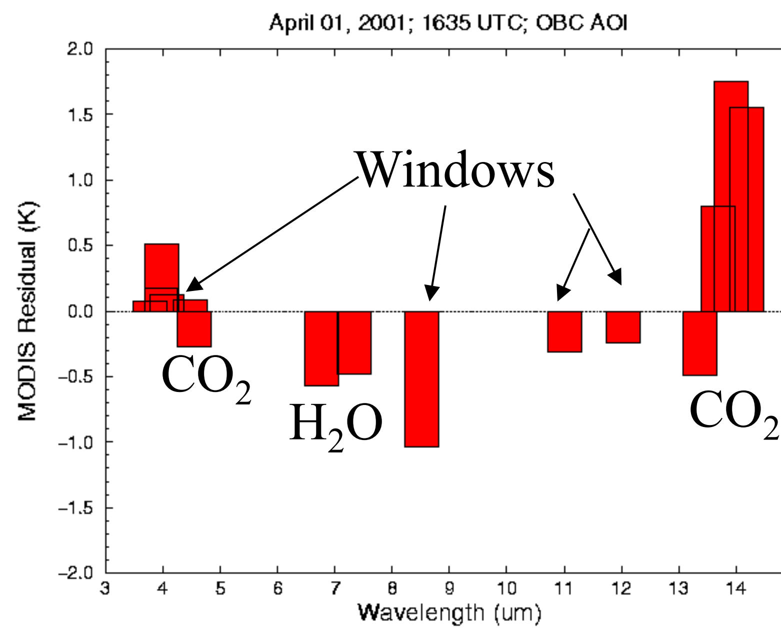

Accounting for Broadband Spectral Response

$$B(\lambda,T) = c_1 / \{ \lambda^5 [e^{c_2/\lambda T} - 1] \}$$

Summing the Planck function over a spectral response function SR (λ) can be approximated

$$\Sigma B(\lambda, T)\, SR(\lambda) = B(\lambda_{eff},T) = c_1 / \{ \lambda_{eff}^5 [e^{c_2/\lambda_{eff}(a+bT)} - 1] \}$$

Adjusted brightness temperature accounts for spectral smearing of the Planck function.

MODIS NEdR Estimate

Band 20	3.7 um	.007 mW/m2/ster/cm-1
Band 21	3.9	.02
Band 22	3.9	.04
Band 23	4.0	.025
Band 24	4.45	.03
Band 25	4.5	.045
Band 27	6.7	.08
Band 28	7.3	.07
Band 29	8.6	.25
Band 30	9.7	.2
Band 31	11.0	.3
Band 32	12.0	.3
Band 33	13.3	.4
Band 34	13.6	.6
Band 35	13.9	.4
Band 36	14.2	.5

Based on Earth Scene Data Day 01153, 20:10 UTC Clear scenes of the Pacific Ocean

Note: Some SG present in MWIR Used 150 x 28 box (420 data points per detector)

MODIS Terra

Performance Issue	Cloud Mask Impact	Action
Band 26 Striping	1.38 um cirrus detection over land	Developed destriping process based on B5 data
S/MWIR Electronic Crosstalk	1.38 um cirrus detection	detector biases adjusted (11/1/00) to reduce effect
Elevated Background Signal in Band 26	1.38 um cirrus detection over land	B5-based OOB correction developed
Thermal IR Band Striping (mirror side and detector)	Difference tests, spatial variability test	Develop detector and mirror side normalizers

MODIS Terra
cont.

Performance Issue	Cloud Mask Impact	Action
SWIR Band Subsample Departure	Thick aerosol (band 7), shadow (band 5) detection	SRCA data set analysis in June/July, ‘01
Saturation in Band 2	Detection of thick cloud over water; sunglint regions	Identify surrogate band when B2 saturates (e.g. B1)

MODIS Aqua

Performance Issue	Cloud Mask Impact	Action
Band 6 Detector Failures	Snow detection	Identify surrogate snow detection band (B7?)
Band 2 Saturation	Detection of thick cloud over water; sunglint regions	Identify surrogate band when B2 saturates (e.g. B1)
S/MWIR Electronic Crosstalk	1.38 um cirrus detection	Pre-launch tests suggest elec xtalk is much smaller on FM1 than PFM
Thermal IR band detector, mirror side striping	Causes striping in difference tests, affect spatial variability	High quality non-linearity info.; post-launch normalization?

MODIS Band 27 (6.7 μm), 2001-06-04 16:45 UTC

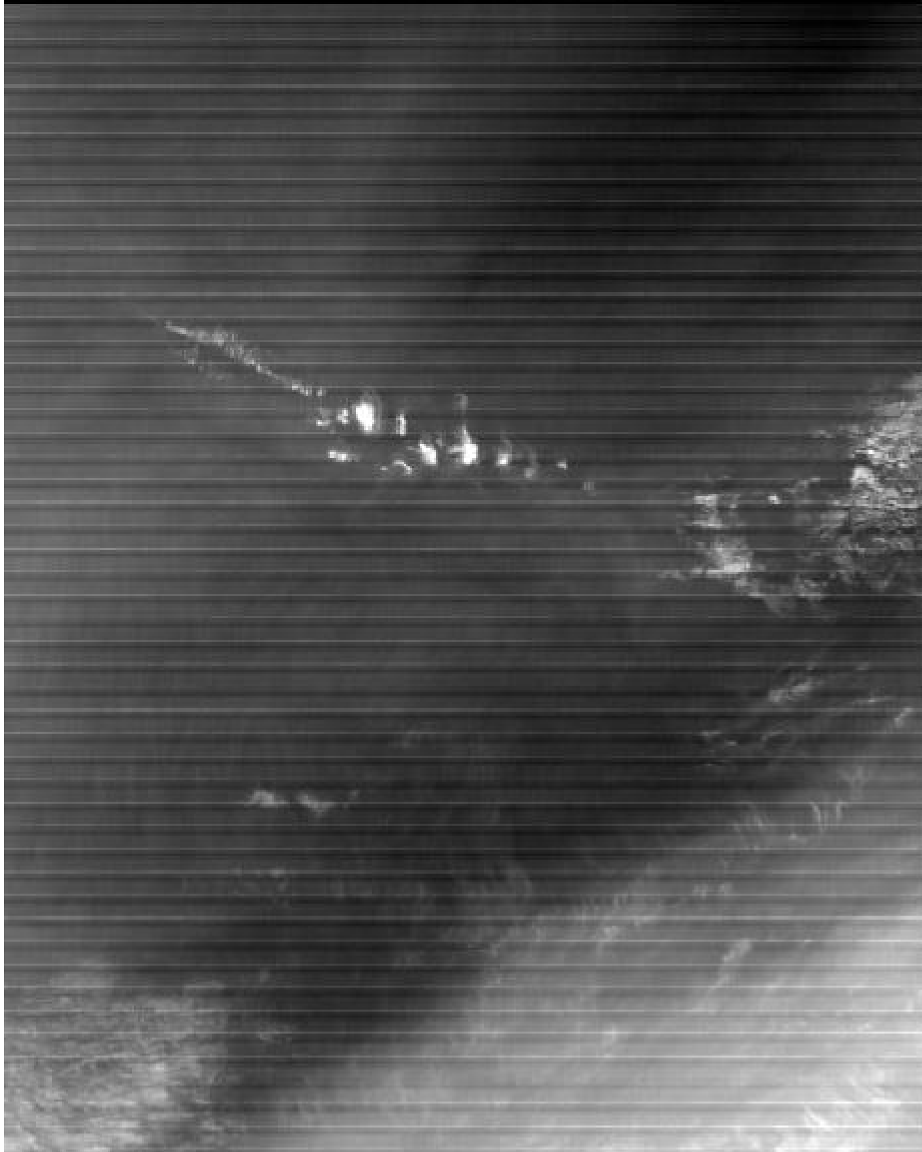

Original L1B (V003)

Destriped

MODIS L1B Accuracy Assessment

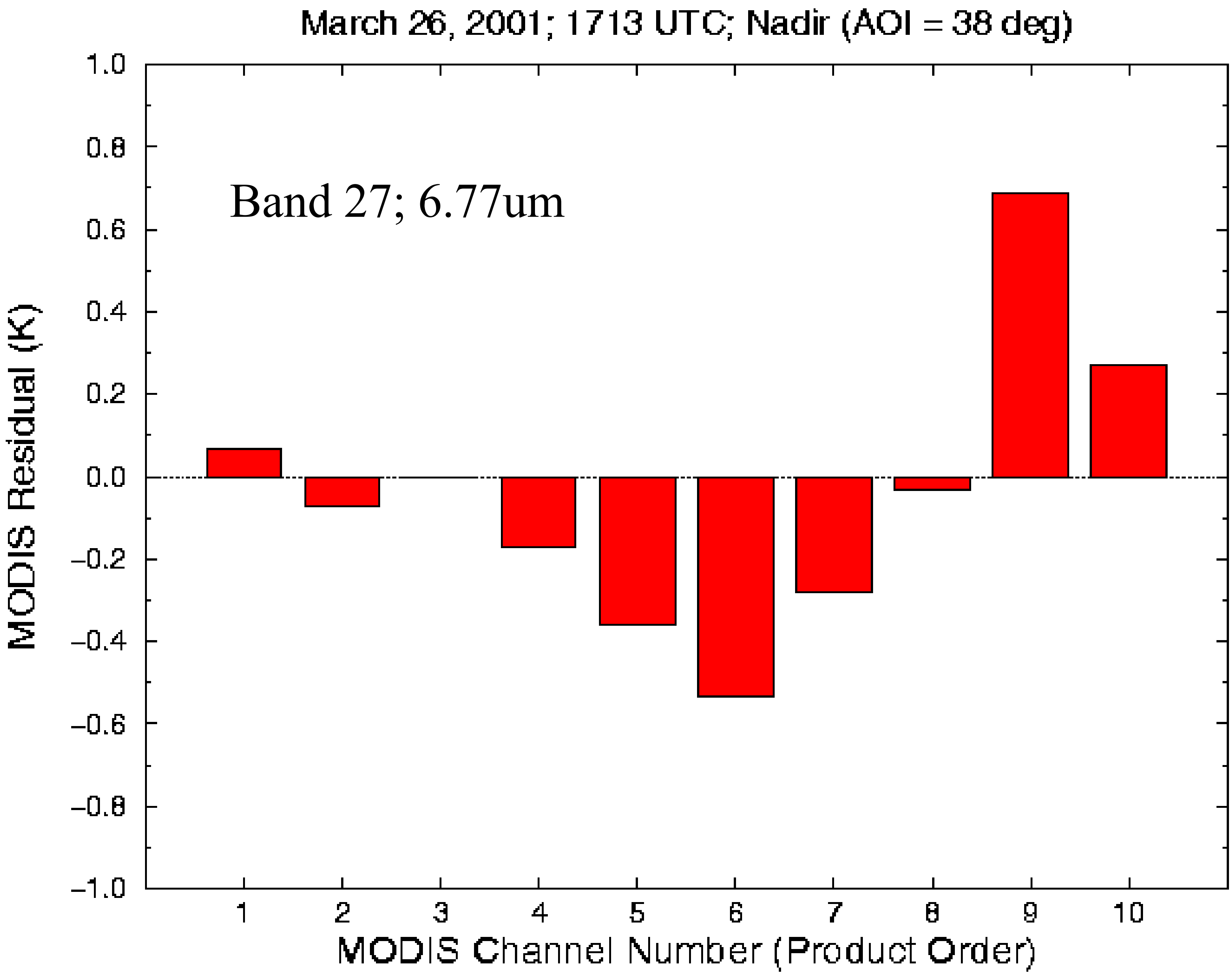

Band 34

Detector Number (Product Order)	RMS (mW/m^2 sr cm^{-1})
1	.46725
2	.40609
3	.51104
4	.43430
5	.73425
6	1.0260
7	1.2547
8	1.1700
9	.56228
10	.35423

Noisy Detectors (5–8)

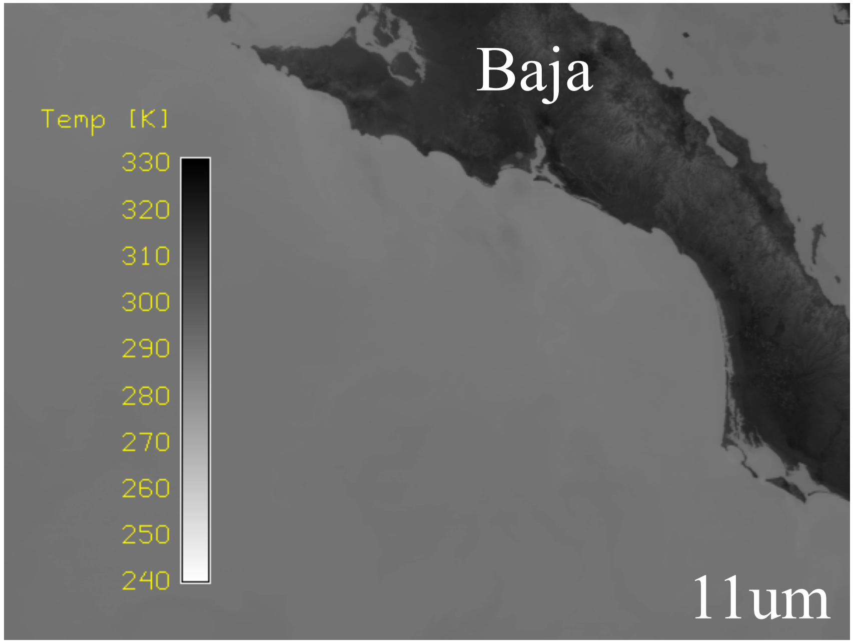

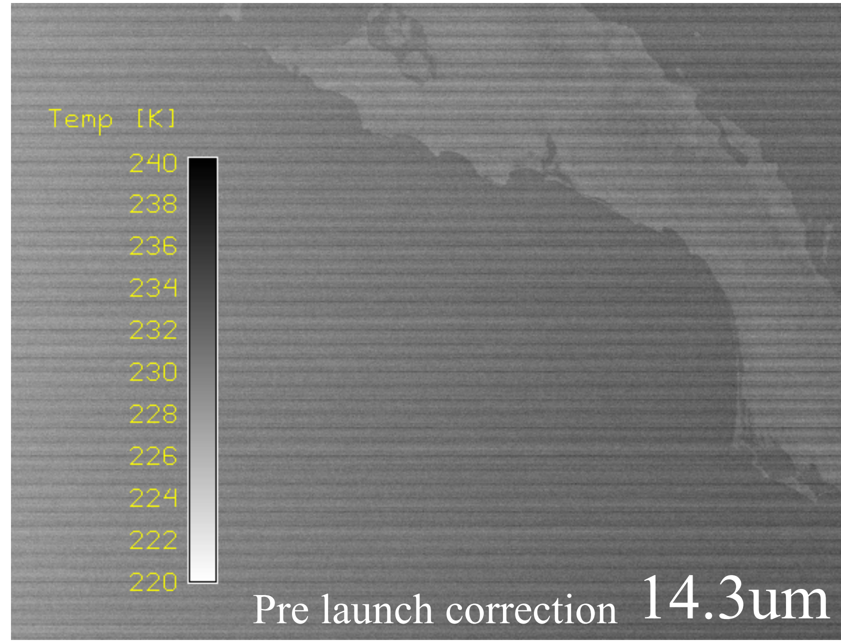

Considerable effort required to tune the correction of the optical leak at 11um for MODIS. Estimated accuracy limited to 1-2% by residual optical crosstalk influence in atmospheric bands.